First order phase transition in the D3-D7 model from the point of view of the fermionic spectral functions

Xian-Hui Ge,[1,*] Shuta Ishigaki,[1,†] Sang-Jin Sin,[2,‡] and Taewon Yuk[2,§]
[1]*Department of Physics, Shanghai University, Shanghai 200444, China*
[2]*Department of Physics, Hanyang University, Seoul 04763, Korea*

(Received 29 March 2024; accepted 13 May 2024; published 8 July 2024)

We consider the D3-D7 model and use the spectral function of a probe fermion on D7 to analyze the first order phase transition from the black-hole embedding phase to another black-hole embedding phase in the presence of the finite density and temperature. From the fermionic spectral functions, we study the temperature dependence of the decay rate, and we observe various phenomena that support the first order phase transition including jump in it at the critical temperature that corresponds to the first order phase transition.

DOI: 10.1103/PhysRevD.110.026003

I. INTRODUCTION

Shortly after the AdS/CFT correspondence [1–3] was established, the method has been applied to investigate quantum chromodynamics (QCD) and condensed matter physics of strongly correlated systems widely. One of the benefits of the holographic method is that it allows us to study strongly coupled quantum many-particle systems easily even for the system with finite temperature and finite density effects.

The D3-D7 model [4] is one of the top-down models that has been used widely for such a purpose. The background Schwarzschild-AdS$_5 \times$ S^5 spacetime generated from the D3-branes and the probe D7-brane play roles of the thermal reservoir and charged particle system, respectively. The solutions and behavior of the probe brane in the black-hole spacetime, i.e., finite-temperature cases, were studied by Refs. [5–8]. The system has intricate dependence on the parameters exhibiting the phase transitions. One of the solutions, that the probe brane falls into the black-hole horizon, called black-hole embedding, is interpreted as a deconfinement phase of the quarks or metallic phase of the electrons. The authors of Refs. [5,6] found that there are two different phases of the brane embeddings where the D7-brane touches the black-hole horizon, and, as the density increases, there is a jump in the position of the horizon touching point. The brane in a phase named the BH-I phase bends sharper than the brane in another phase named the BH-II phase. The difference of these phases should have a physical interpretation from the viewpoint of the boundary field theory. Since the black-hole touching configurations should be related to the metallic phase, the phase transition should be related to the metal-to-metal phase transition. Therefore, we can expect that certain phase transition in spectrum or transport property. However, the details of the physical meaning of the two phases has been completely obscure.

Although the spectral functions of bosonic fluctuations in this model were studied in Refs. [9–12], the fermionic spectral functions are a more interesting quantity, because they can be directly measured by angle-resolved photoemission spectroscopy experiments. In this work, therefore, we consider a probe fermion field living on the D7 model and compute the fermionic spectral function. The fermion spectral functions for the bottom-up model were already studied extensively [13–19]. However, the fermion spectral function in fundamental representation with the D3-D7 model has not been studied much. Since we want the fermion to provide the matter density, the natural candidate of the fermionic field in the D7-brane is the fermionic degree of freedom coming from the D3-D7 string [20] rather than the mesino [21–25].

In this study, we consider a toy model with a fermionic field ψ to utilize the D7's induced metric. One should notice that the brane configuration is coming from the D7-brane and, therefore, common to all the fluctuations of it. Our fermionic field is coupled to the bulk U(1) gauge fields as in the bottom-up models, e.g., [13,14]. For a given embedding, we obtain the fermionic spectral functions by solving the Dirac equation. Because we consider the system

*gexh@shu.edu.cn
†shutaishigaki@shu.edu.cn
‡sangjin.sin@gmail.com
§tae1yuk@gmail.com

in the black-hole geometry, the Fermi surface is always smeared. We can locate the smeared Fermi surface by the pole or singularity position of the spectral function, and the density of state has a Drude-like peak at zero frequency with a finite width. We study the behavior of the decay width of the fermion for various temperatures. The width exhibits a universal behavior of holographic models at high enough temperature. In a specific range of the parameters, it has a jump in the temperature associated with the first order phase transition of the background D3-D7 system. We believe that this is universal for all other brane models.

From the fermionic spectral functions, we study the temperature dependence of the decay rate, and we observe a jump in it at the critical temperature that corresponds to the first order phase transition. We found that the jump in the decay rate mimics that in the resistivity data in a recent heavy fermion material. If the material were weakly interacting, this would be natural, but it is unclear why this similarity holds in the strongly interacting case, and understanding this is left as an future work.

This paper is organized as follows. We present a review of the D3-D7 model with finite density in Sec. II. In Sec. III, we consider a toy model of the fermionic field probing the background D3-D7-brane system, and we study the spectral functions of the dual operator. We also study the width of the spectral functions and its temperature dependence, and we compare it with the resistivity data. We discuss and conclude in Sec. IV.

II. A REVIEW: D3-D7 MODEL WITH FINITE DENSITY

A. Background solutions

We briefly review the D3-D7 model [4] with finite baryon density and temperature following [5,6], where the authors showed phase transitions from a black-hole phase to another black-hole phase. The action of the D7 probe brane is given by the following Dirac-Born-Infeld action:

$$S_{\mathrm{DBI}}[X,A] = -\tau_7 \int \mathrm{d}^8\xi \sqrt{-\det[h_{ab} + (2\pi\alpha')F_{ab}]}, \tag{1}$$

where τ_7 is the tension of the D7-brane and h_{ab} is the induced metric given by

$$h_{ab} = \frac{\partial X^M}{\partial \xi^a}\frac{\partial X^N}{\partial \xi^b} g_{MN}. \tag{2}$$

ξ^a and X^M are the coordinates of world volume and ten-dimensional bulk, respectively. g_{MN} is the metric of the background ten-dimensional spacetime. We set the background spacetime to Schwarzschild-$\mathrm{AdS}_5 \times \mathrm{S}^5$ spacetime. In isotropic coordinates, the metric can be written as

$$\begin{aligned}\mathrm{d}s^2 = \frac{w^2}{L^2}\left[-\frac{f_1(w)^2}{f_2(w)}\mathrm{d}t^2 + f_2(w)\mathrm{d}\vec{x}^2\right] \\ + \frac{L^2}{w^2}(\mathrm{d}\rho^2 + \rho^2\mathrm{d}\Omega_3{}^2 + \mathrm{d}w_5{}^2 + \mathrm{d}w_6{}^2),\end{aligned} \tag{3}$$

where $f_1(w) = 1 - w_h^4/w^4$, $f_2(w) = 1 + w_h^4/w^4$, $w^2 = \rho^2 + w_5^2 + w_6^2$, and $\mathrm{d}\Omega_3{}^2$ is the line element of the unit three-sphere.[1] The Hawking temperature T is related to the location of the horizon w_h by $w_h = \pi T/\sqrt{2}$. For convenience, we use the following metric:

$$\begin{aligned}\mathrm{d}s^2 = \frac{L^2}{u^2}\left[-\frac{f(u)^2}{\tilde{f}(u)}\mathrm{d}t^2 + \tilde{f}(u)\mathrm{d}x^2\right] + L^2\frac{\mathrm{d}u^2}{u^2} \\ + L^2(\mathrm{d}\theta^2 + \sin^2\theta\mathrm{d}\varphi^2 + \cos^2\theta\mathrm{d}\Omega_3{}^2),\end{aligned} \tag{4}$$

where $f(u) = 1 - u^4/u_h^4$ and $\tilde{f}(u) = 1 + u^4/u_h^4$. u and w are related by $u = 1/w$. w_5, w_6, and ρ are related to θ, φ, and u by

$$\begin{aligned}w_5 = u^{-1}\sin\theta\cos\varphi, \qquad w_6 = u^{-1}\sin\theta\sin\varphi, \\ \rho = u^{-1}\cos\theta,\end{aligned} \tag{5}$$

respectively. The other nonzero supergravity field is a Ramond-Ramond five-form flux

$$\begin{aligned}F_{(5)} = -\frac{4}{L^4u^5}f(u)\tilde{f}(u)\mathrm{d}t\wedge\mathrm{d}x\wedge\mathrm{d}y\wedge\mathrm{d}z\wedge\mathrm{d}w \\ + 4L^4\mathrm{vol}(\mathrm{S}^5),\end{aligned} \tag{6}$$

where $\mathrm{vol}(\mathrm{S}^5)$ is the volume form of the unit five-sphere. It satisfies the self-dual constraint in the type IIB supergravity: ${}_*F_{(5)} = F_{(5)}$.

We choose the world volume coordinates as $\xi^a = (t, \vec{x}, u, \Omega_3)$; then the transverse directions are θ and φ. Since φ can be set to zero by virtue of a symmetry, $\theta(u)$ describes an embedding of the probe brane. The induced metric is given by

$$\begin{aligned}h_{ab}\mathrm{d}\xi^a\mathrm{d}\xi^b = \frac{1}{u^2}\left[-\frac{f(u)^2}{\tilde{f}(u)}\mathrm{d}t^2 + \tilde{f}(u)\mathrm{d}x^2\right] \\ + \left(\frac{1}{u^2} + \theta'(u)^2\right)\mathrm{d}u^2 + \cos^2\theta\mathrm{d}\Omega_3{}^2.\end{aligned} \tag{7}$$

We set $L = 1$ for simplicity. F_{ab} is the field strength of the world volume U(1) gauge fields A_a. We consider an ansatz for the gauge fields as $A_a\mathrm{d}\xi^a = A_t(u)\mathrm{d}t$ so the nonzero components of the field strength are only F_{tu} and F_{ut}. Writing $S_{\mathrm{DBI}} = \int \mathcal{L}$, the Lagrangian density is given by

[1]The radial coordinate w can be written as $w^2 = \sum_{i=1}^6 w_i{}^2$ and $\rho^2 = \sum_{i=1}^4 w_i{}^2$. The coordinate w is related to the Schwarzschild coordinate r by $w^2 = \frac{r^2}{2} + \frac{1}{2}\sqrt{r^4 - r_h^4}$.

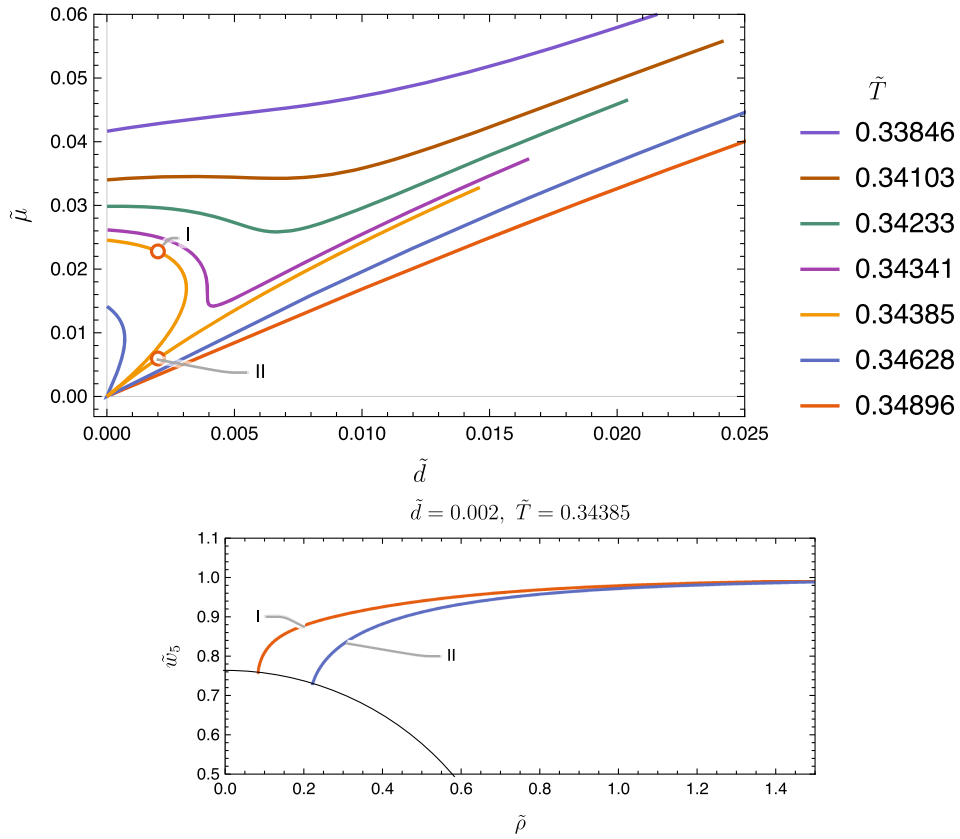

FIG. 1. Top: relation between the density and chemical potential for various temperatures. Bottom: brane embeddings corresponding to I and II in the top panel.

$$\mathcal{L} = -\mathcal{N}\cos^3\theta h_{xx}^{3/2}\sqrt{|h_{tt}|h_{uu} - A_t'(u)^2}, \tag{8}$$

where $\mathcal{N} = \tau_7(2\pi^2)$. A constant of motion d for A_t is given by

$$d = \frac{1}{\mathcal{N}}\frac{\partial\mathcal{L}}{\partial A_t'(u)}. \tag{9}$$

d is related to the charge density in the boundary theory. Solving the equation of motion, we can write

$$A_t'(u) = -duf(u)\sqrt{\frac{1+u^2\theta'(u)^2}{\tilde{f}(u)(d^2u^6+\tilde{f}(u)^3\cos^6\theta(u))}}. \tag{10}$$

A chemical potential μ is obtained by

$$\mu = \int_{u_h}^{0} A_t'(u)\mathrm{d}u = A_t(0) - A_t(u_h). \tag{11}$$

We have set $A_t(u_h) = 0$.

We perform the Legendre transformation to eliminate $A_t'(u)$ from the Lagrangian density (8):

$$\tilde{\mathcal{L}} \equiv \mathcal{L} - A_t'(u)\frac{\partial\mathcal{L}}{\partial A_t'(u)} = -\mathcal{N}\sqrt{|h_{tt}|h_{uu}(d^2 + h_{xx}^3\cos^6\theta)}. \tag{12}$$

The Euler-Lagrange equation of $\tilde{\mathcal{L}}$ gives us the equation of motion for $\theta(u)$:

$$\frac{\partial}{\partial u}\left[-\sqrt{\frac{|h_{tt}|\Xi}{h_{uu}}}\theta'(u)\right] - 3\cos^5\theta\sin\theta h_{xx}^3\sqrt{\frac{|h_{tt}|h_{uu}}{\Xi}} = 0,$$
$$\Xi \equiv d^2 + h_{xx}^3\cos^6\theta. \tag{13}$$

We can solve the equation of motion from $u = u_h$ with a regular condition.[2] For regular solutions, $\theta'(u_h) = 0$ must be satisfied at $u = u_h$. The family of solutions is parametrized by $\theta(u_h)$ and d. The range of $\theta(u_h)$ is $0 \le \theta(u_h) < \pi/2$. $\theta(u)$ has an asymptotic expansion of

$$\theta(u) = m_q u + \theta_2 u^2 + \cdots, \tag{14}$$

at $u = 0$. m_q and θ_2 are related to the quark mass and the quark condensate in the boundary theory, respectively.

[2]In the case of $T = 0$, the analytic solutions for the embedding function and the gauge field are found in Ref. [26].

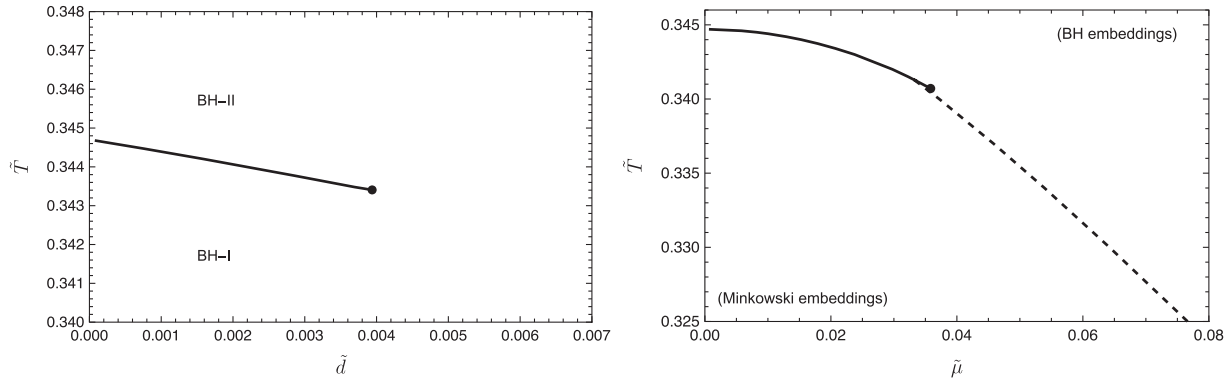

FIG. 2. Phase diagrams of the probe brane. Left: canonical ensemble; i.e., $\tilde{d}$ is a controlling parameter. The black line is the first order phase transition line. The end point at $\tilde{d} = \tilde{d}_c \approx 0.004$ indicates the second order phase transition end point. For $\tilde{d} < \tilde{d}_c$, we call the low- and high-temperature regime as the BH-I and BH-II phase, respectively. Right: grand canonical ensemble; i.e., $\tilde{\mu}$ is a controlling parameter. The black line is the first order phase transition line. The dashed line denotes the second order phase transition line.

[See Eq. (A4).] In the isotropic coordinates, m_q is the separation distance between the probe D7-brane and the D3-branes at the AdS boundary: $w_5(u = 0) = m_q$.

Since the system has a scaling symmetry, we should consider only scale invariants. By taking m_q as a scale, we define scale invariant temperature, chemical potential, and density by

$$\tilde{T} \equiv \frac{T}{m_q}, \qquad \tilde{\mu} \equiv \frac{\mu}{m_q}, \qquad \tilde{d} \equiv \frac{d}{m_q^3}, \tag{15}$$

respectively. We also define scaled isotropic coordinates by $\tilde{w}_5 = w_5/m_q$, $\tilde{w}_6 = w_6/m_q$, and $\tilde{\rho} = \rho/m_q$ for fixed m_q. By definition, $\tilde{w}_5(u = 0)$ is always one.

By solving Eq. (13), we obtain relation between $\tilde{d}$ and $\tilde{\mu}$ for several $\tilde{T}$, as we show in the top panel in Fig. 1. The results agree with those obtained in Ref. [6]. In the range of $0.34341 < \tilde{T} < 0.34468$, $\tilde{\mu}$ becomes a multivalued function of $\tilde{d}$, and, hence, there are multiple solutions for given $\tilde{d}$ at $\tilde{T}$. In the bottom panel in Fig. 1, we show the corresponding embeddings labeled by I and II at $\tilde{d} = 0.002$ and $\tilde{T} = 0.34385$.[3] We refer to the upper solution and the lower solution in the bottom panel in Fig. 1 as BH-I and II embedding, respectively. The first order phase transition occurs in such a case. The transition points are determined from the free energy or the Maxwell construction as we discuss in the Appendix. At $\tilde{T} = 0.34341$, the system has the second order phase transition when $\tilde{d} = 0.0039385$. At a temperature out of the above range, there is a crossover.

The phase structures are summarized as phase diagrams in Fig. 2. The phase structure changes depending on whether $\tilde{d}$ or $\tilde{\mu}$ is treated as a controlling parameter, in other words, considering a canonical ensemble or a grand canonical ensemble, respectively. We show the first order transition line as the black curve and the second order phase transition line as the black dashed line. In the canonical ensemble, the ranges of the phase transition are $0.34341 < \tilde{T} < 0.34468$ and $0 < \tilde{d} < \tilde{d}_c = 0.0039385$. In this case, the embeddings are always given by the BH embeddings, but it is divided by the first order phase transition line in $\tilde{T}$ for $\tilde{d} < \tilde{d}_c$. We call the low- and high-temperature regime in $\tilde{d} < \tilde{d}_c$ as the BH-I and BH-II phase, respectively. The BH-I and II embeddings shown in the bottom panel in Fig. 1 belong to the BH-I and II phase, respectively. In the grand canonical ensemble, there are brane solutions without touching the black-hole horizon called Minkowski embeddings. The Minkowski embeddings are realized with vanishing density. We do not focus on such solutions in this study.

III. PROBING BY A FERMIONIC FIELD

In this section, we consider dynamics of a spinor field probing the background D7-brane's world volume. Our fermion is coming from the string connecting D3-D7 rather than the D7-D7, unlike the mesino. In the scaling limit where D3's disappear to be the AdS gravity, the string connects D7 and horizon, and the low-energy physics of the string becomes that of the Dirac fermion in fundamental $U(N_f)$ representation on D7 world volume. Here, we set $N_f = 1$. This string as a fermion was also utilized in [20] to argue that, in the presence of the finite density of the fermion, only black-hole embedding (BHE) is allowed. Here, our transition is from BHE to BHE. The Dirac fermion in fundamental representation is charged and, therefore, should contribute to the conductivity. As a first step of the study of the fermionic spectral function in the

[3]Since the solution at the middle point of the $\tilde{\mu} - \tilde{d}$ curve will be unstable, we do not focus on it in this paper.

D3-D7 model, we consider the fermion's action governed by the five-dimensional part of the induced metric (7) ignoring the three-sphere part of induced metric to avoid the technical complication. This should not change the essential features, since the shape of the brane is already encoded in the five-dimensional model, and extra factors of $\cos\theta$ in the measure should not change the qualitative features of the theory.

We now consider the following simplified model:

$$S_{\text{spinor}} = i\int \mathrm{d}^5x\sqrt{-\det h_{\mu\nu}}\bar{\psi}(\gamma^\mu\mathcal{D}_\mu - m)\psi + S_{\text{bou}}, \quad (16)$$

where $h_{\mu\nu}$ is the five-dimensional part of the induced metric, that is,

$$h_{\mu\nu}\mathrm{d}x^\mu\mathrm{d}x^\nu = \frac{1}{u^2}\left[-\frac{f(u)^2}{\tilde{f}(u)}\mathrm{d}t^2 + \tilde{f}(u)\mathrm{d}x^2\right] + \left(\frac{1}{u^2} + \theta'(u)^2\right)\mathrm{d}u^2. \quad (17)$$

$\mathcal{D}_\mu = \nabla_\mu - iqA_\mu$ is a gauge covariant derivative, and S_{bou} is the boundary action which will be specified later. Notice that the covariant derivative is also defined with respect to the five-dimensional metric $h_{\mu\nu}$. Using the spin connection with respect to $h_{\mu\nu}$, it can be written as

$$\nabla_\mu = \partial_\mu + \frac{1}{8}\omega_\mu{}^{\underline{\nu\rho}}[\gamma_{\underline{\nu}}, \gamma_{\underline{\rho}}], \quad (18)$$

where γ^μ denotes gamma matrices in the curved spacetime and $\gamma_{\underline{\mu}}$ are gamma matrices in the tangent space that will be defined as follows: It can be written as $\gamma^\mu = e^\mu{}_{\underline{\mu}}\gamma^{\underline{\mu}}$, where $e^\mu{}_{\underline{\mu}}$ is the inverse matrix of vielbein $e_\mu{}^{\underline{\mu}}$, which satisfies $e_\mu{}^{\underline{\mu}}e_\nu{}^{\underline{\nu}}\eta_{\underline{\mu\nu}} = h_{\mu\nu}$, and $\gamma^{\underline{\mu}}$ is the gamma matrices in the tangent space. The gamma matrices in the five-dimensional spacetime can be chosen as

$$\gamma^{\underline{0}} = \sigma^1\otimes i\sigma^2, \quad \gamma^{\underline{1}} = \sigma^1\otimes\sigma^1, \quad \gamma^{\underline{2}} = \sigma^1\otimes\sigma^3,$$
$$\gamma^{\underline{3}} = \sigma^2\otimes I_2, \quad \gamma^{\underline{u}} = \sigma^3\otimes I_2, \quad (19)$$

where σ^1, σ^2, and σ^3 are the Pauli matrices. Then, $\psi(x^\mu)$ is written as a four-components spinor field.

The equation of motion is the Dirac equation

$$(\gamma^\mu\mathcal{D}_\mu - m)\psi(t,\vec{x},u) = 0. \quad (20)$$

Substituting the five-dimensional metric, we can write

$$\gamma^\mu\mathcal{D}_\mu = e^\nu{}_{\underline{\mu}}\gamma^{\underline{\mu}}(\partial_\mu - iqA_\mu) + \frac{1}{4}e^u{}_{\underline{u}}\gamma^{\underline{u}}\partial_u\ln(-\det(h_{\mu\nu})h^{uu}). \quad (21)$$

Considering the following transformation:

$$\psi(x^\mu) = (-\det(h_{\mu\nu})h^{uu})^{-1/4}\phi(x^\mu), \quad (22)$$

we obtain the following equation:

$$[e^\nu{}_{\underline{\mu}}\gamma^{\underline{\mu}}(\partial_\nu - iqA_\nu) - m]\phi(x^\mu) = 0. \quad (23)$$

We decompose the four-component spinor field ψ as follows:

$$\psi(x^\mu) = \psi_+(t,\vec{x},u) + \psi_-(t,\vec{x},u), \quad (24)$$

where $\psi_\pm$ are projected by $\psi_\pm = P_\pm\psi$ with $P_\pm = (1\pm\gamma^u)/2$. According to Ref. [15], the asymptotic behaviors of the spinors are written as

$$\psi_+ = \psi_+^{(0)}u^{\Delta_-} + \psi_+^{(1)}u^{1+\Delta_+} + \cdots,$$
$$\psi_- = \psi_-^{(0)}u^{\Delta_+} + \psi_-^{(1)}u^{1+\Delta_-}\cdots, \quad (25)$$

where $\Delta_\pm = 2\pm m$. $\psi_\pm^{(0)}$ and $\psi_\pm^{(1)}$ are related to the source and fermionic operator with the scaling dimension of Δ_+, respectively. To obtain retarded responses, we also impose the ingoing-wave boundary condition at the black-hole horizon. In order to compute the Green's function, we need to fix the boundary action. We employ

$$S_{\text{bdy}} = \lim_{u\to\varepsilon}\frac{i}{2}\int \mathrm{d}^4x\sqrt{-hh^{uu}}\bar{\psi}\psi, \quad (26)$$

where ε is a small positive cutoff ε and $\bar{\psi}_+ = \psi^\dagger\gamma^0$.[4] This choice of the boundary term is known as the standard quantization [27]. The retarded Green's function is obtained by

$$G^{\text{R}}(k) = i\mathcal{S}\gamma^0 = \frac{2m+1}{k^2}(\gamma\cdot k)\mathcal{T}\gamma^0, \quad (27)$$

where $\mathcal{S}$ and $\mathcal{T}$ are defined, respectively, by

$$\psi_-^{(1)} = \mathcal{S}\psi_+^{(0)}, \quad \psi_+^{(1)} = \mathcal{T}\psi_-^{(0)}. \quad (28)$$

The Green's function has a scaling dimension of $-2m$. We can also derive the flow equation for $G^{\text{R}}(k,u)$ from the Dirac equation, as those in Ref. [19]. In the following section, we compute the result by solving the flow equation.

For later convenience, we define spectral function by

$$A(\omega,|\vec{k}|) = -\mathrm{Im}\,\mathrm{tr}\,G^{\text{R}}(\omega,\vec{k}). \quad (29)$$

[4]A similar boundary action was employed in [23] for the top-down model.

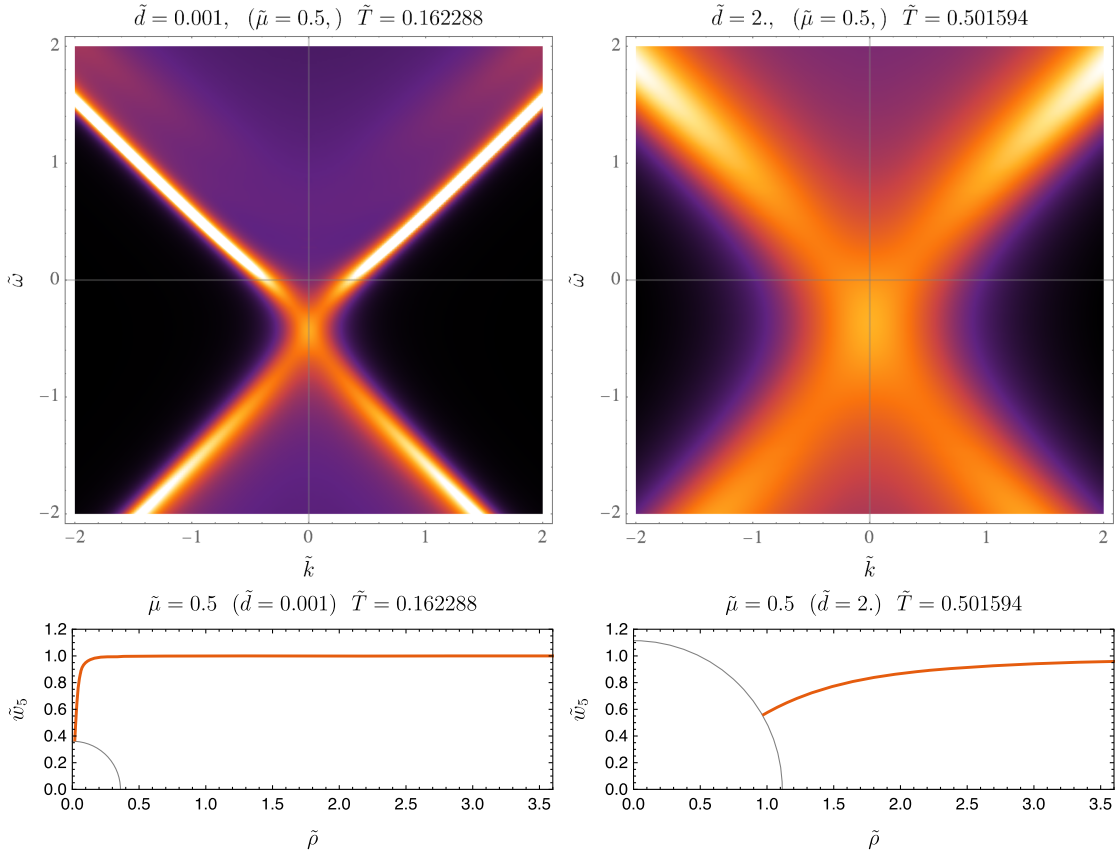

FIG. 3. Top: spectral functions $\tilde{A}(\tilde{\omega}, \tilde{k})$ for two setups. We set $m = 0.2$. Bottom: brane embeddings corresponding to the top panels, respectively. The black circle shows the location of the black-hole horizon.

Since the system is isotropic, $A(\omega, k)$ depends only on $k \equiv |\vec{k}|$. We also define a scaled spectral function

$$\tilde{A}(\tilde{\omega}, \tilde{k}) = m_q^{2m} \times A(m_q\tilde{\omega}, m_q\tilde{k}). \tag{30}$$

A. Spectral function

We show the spectral functions of the two embeddings with $\tilde{\mu} = 0.5$ in Fig. 3. The left panel in Fig. 3 corresponds to a solution in the BH-I phase, and the right panel in Fig. 3 corresponds to a solution in the crossover region in Fig. 2. The spectral function of the left panel in Fig. 3 is similar to those obtained in Ref. [28]. In both cases, the Dirac points are shifted by μ. It is also similar to the results of Refs. [13,28]. As T increases, the peaks of the spectral function are smeared.

It is considered that the Fermi level is located at $\omega = 0$. The intersection between the peaks and the horizontal axis is considered as the Fermi surface, but it is smeared at finite temperatures. In the following, we define the Fermi momentum of the smeared Fermi surface and the width of the Drude-like peak.

B. Smeared Fermi surface

At finite temperatures, the Fermi surface is smeared, so we can no longer define sharp Fermi momentum k_F. However, we can still define an analog of k_F from the "pole" of the retarded Green's function there.[5] In normal isotropic metals, k_F satisfies $E(k_F) = \mu$, where $E(k)$ denotes the dispersion relation. The spectral function in the noninteracting theory should have a delta function peak at the Fermi momentum, and the Green's function has a pole there.

At finite temperatures of our interacting theory, the spectral function is smeared, and we assume that the pole is located on the lower half complex ω plane with a finite distance from the real axis so that the Green's function has the following structure:

[5]Another possible definition of the smeared Fermi momentum is using local maximum of the spectral function. It will be expressed by

$$\{k_F'\} = \arg_k \max A(\omega = 0, k).$$

It determines only k_F'. The width will be measured from the peak. However, we do not use this definition of the smeared Fermi surface in this study.

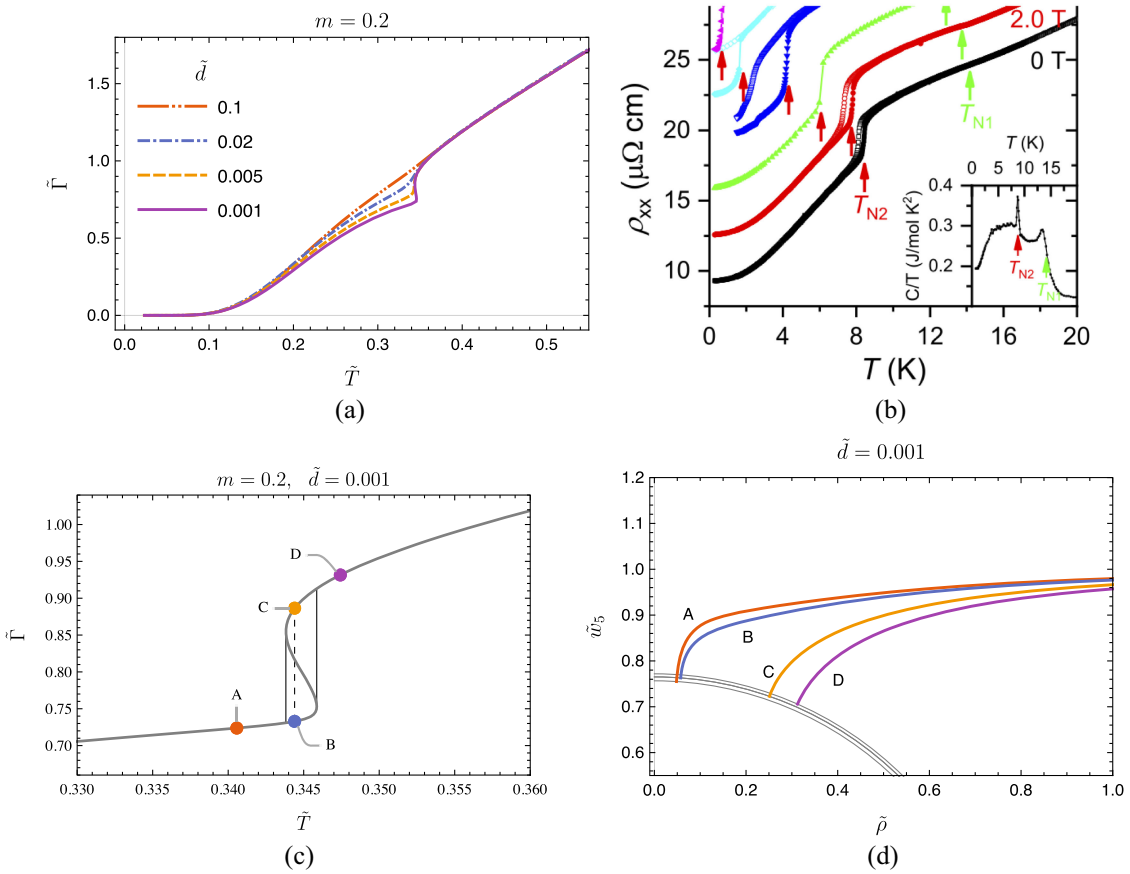

FIG. 4. (a) Γ vs T for various densities. (b) Resistivity data in a heavy fermion material. Curiously, both (a) and (b) show the jump from a linear T to another linear in T. In (c), the vertical dashed line denotes the T_c. The points labeled by A–D correspond to the embeddings in the right panel, respectively. In (d), the gray circles denote the black-hole horizon at each temperature. The embeddings B and C have a common temperature $\tilde{T} = \tilde{T}_c$. (b) is from [29].

$$\mathrm{tr}\, G^{\mathrm{R}}(\omega, k) = \frac{Z_\Gamma}{\omega - k + k'_F + i\Gamma/2} + \cdots, \tag{31}$$

where Γ is the width, i.e., the decay constant. Z_Γ is a constant residue. k'_F is also a positive real constant which can be understood as a center of smeared Fermi momentum. Taking the inverse of $\mathrm{tr}\, G^{\mathrm{R}}$ and evaluating it at $(\omega, k_F) = (-i\Gamma/2, k'_F)$, we obtain the equation

$$\frac{1}{\mathrm{tr}\, G^{\mathrm{R}}(\omega = -i\Gamma/2, k = k'_F)} = 0. \tag{32}$$

We can determine k'_F and Γ by solving this complex-valued equation. In the following, we will study the behavior of Γ by using Eq. (32).

C. T dependence of the decay rate

From Eq. (32), we compute Γ for various temperatures. We define the scaled width by $\tilde{\Gamma} \equiv \Gamma/m_q$. Figure 4 shows the width Γ as functions of the temperature T for various values of scaled density and chemical potential, $\tilde{d}$ and $\tilde{\mu}$. In both cases, we find that Γ is linear in T at high temperatures. For sufficiently low density, the curves have a small multivalued region around $T = 0.35 m_q$ corresponding to the multivalued results shown in Fig. 1(a). When T is taken to be sufficiently small, Γ depends on T as $\Gamma \approx \gamma e^{-\alpha/T}$ with a positive constant α near zero temperature. These behaviors along the temperature may appear in various holographic models; e.g., see Ref. [17].

Figure 4(c) shows an enlarged view of Fig. 4(a) around the phase transition point for $\tilde{d} = 0.001$. The dotted vertical dashed line shows the transition point at $T = T_c = 0.34440$. In adiabatic measurements, it is anticipated that the results will exhibit a discontinuity between points B and C, with the intermediate S-shaped branch being omitted. We show the brane embeddings for the points labeled by A–D in Fig. 4(d). The points A and B belong to the BH-I phase, and C and D belong to the BH-II phase.

In passing, we point out that our result in decay rate showing the first order transition from a black-hole

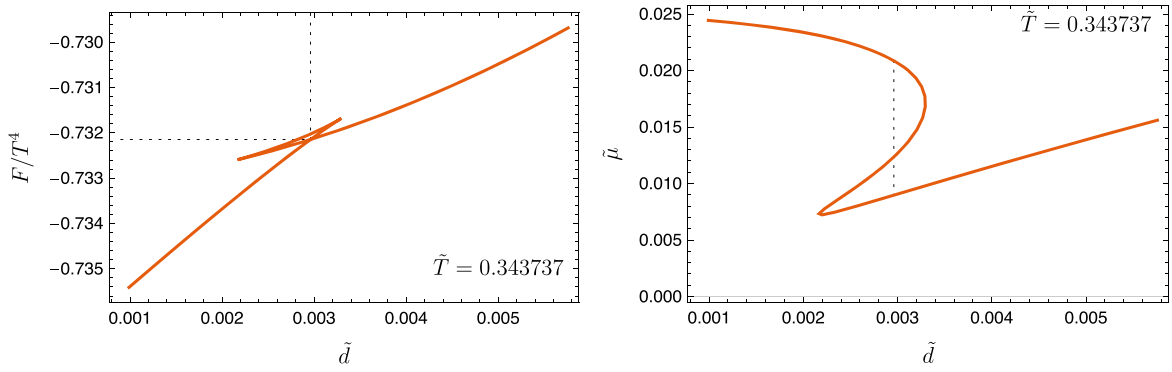

FIG. 5. Left: free energy vs density at $\tilde{T} = 0.343737$. The dotted lines shows the first order phase transition point at $\tilde{d} \approx 0.003$. Right: $\tilde{\mu}$ vs $\tilde{d}$. The vertical dotted line shows the phase transition point.

embedding phase to another black-hole embedding phase exhibits a qualitative similarity to the experimental measurement of the resistivity in a Kondo compound [29,30], some of which is captured in Fig. 4(b) showing the experimental result of Ref. [29]. The Kondo compound also exhibit a drop of the first order phase transition in the resistivity, and the data certainly suggest that there is a first order phase transition from a strange metal to another strange metal with different slope, although at the present time the microscopic reason for such a transition is not known. However, we need to make a caution. In weakly interacting cases, comparing the resistivity and the decay rate is justified by the Drude theory, but here there is no established reason to do so. Therefore, understanding the similarity is left as a future work of the community. The presence of the first order transition is common in the brane system and material system, and there is a further similarities list below.

(1) The first is the specific heat whose data are in the inset in Fig. 4(b). One sees that there is a sharp peak at the position of the phase transition. It is well consistent with our calculation, because from Figs. 5 (left) and 6 (left), the free energy has slope difference around the phase transition point. Since the specific heat is second derivative the free energy, $C_V = -T\frac{\partial^2 F}{\partial T^2}$, our free energy calculation shown in the Appendix implies the delta function peak in C_V vs T. Notice that the figure is for F/T^4 vs d/T^3 with fixed T/m_q, so that the same first order nature appears for fixed density with varying T. Such a peak is the main feature of the data in the figure inset in Fig. 4(b).

(2) We also find that the presence of the hysteresis at zero magnetic field is also consistent with our calculation presented in Fig. 4(c).

These indicate that the similarity of the brane embedding and the dynamics of the heavy fermion is something we might utilize in the future study. But we should not consider our present theory as a serious explanation of the phenomena at all. It is not the purpose of this paper but an observation of similarity.

We have to make a few remarks: First, our model of the probe fermion is a simplified model where the extra

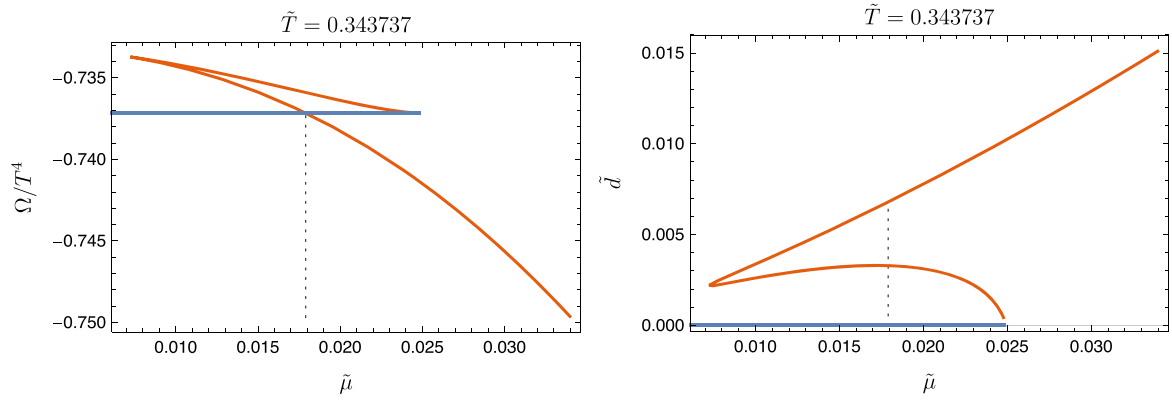

FIG. 6. Left: grand potential vs chemical potential at $\tilde{T} = 0.343737$. The dotted line shows the first order phase transition point at $\tilde{\mu} \approx 0.018$. The red and blue curves show results in the BH and the Minkowski embedding, respectively. Right: $\tilde{d}$ vs $\tilde{\mu}$. The vertical dotted line shows the phase transition point.

dimension of the three-sphere is neglected. The treatment of the extra dimensions in the brane should be improved in the future if one truly wants a top-down theory.

IV. DISCUSSIONS

In this paper, we study the fermionic spectral function in the D3-D7 model by considering the toy model of the probe spinor field. From the spectral function, we investigate the behavior of the decay rate for varying temperature. Most of the quantity we calculated shows a remnant of the first order phase transition. We find that the decay rate also shows the dropping behavior corresponding to the first order phase transition between the BH-I and BH-II phases. We also mentioned the similarity of the decay rate to the transport data, although its ground is unclear to us from the strongly coupled system point of view.

It may be partially related to the puzzle in the holography: While the transport coefficients calculated with holographic method are too sensitive to the details of the background, those in the metallic phase of real condensed matter with strong correlations are universal which exhibit the linear in T resistivity. It may be useful to remind that the fermion width is shown to be universal [19].

The first order phase transition is one of the characteristic behaviors in the brane models. While the holographic superconductors exhibit only the second order phase transition, the brane models often show the first order phase transition. Our original motivation was to understand the physical meaning of the first order phase transition between the two black-hole phases using the probe fermion.

We expect that there is a common mechanism existing for the first order transition between two dissipative phases in both the D3-D7 model and those Kondo compounds. As far as we know, the physical meaning of the low-temperature phase and the first order phase transition is still not understood in the material science point of view. It would be very interesting if we can reveal the above point by further investigation.

ACKNOWLEDGMENTS

We thank the Asia pacific center for theoretical physics for the hospitality during the focus program, where part of this work was discussed. This work is partly supported by National Science Foundation of China (No. 12275166 and No. 12147158). S.-J. S. and T. Y. are supported by National Research Foundation of Korea Grants No. NRF-2021R1A2B5B02002603, No. NRF-2022H1D3A3A 01077468, and by the Basic Research Laboratory (BRL) support program of NRFKR with No. RS-2023-00218998.

APPENDIX: THE FREE ENERGY AND PHASE TRANSITION POINTS

In this section, we discuss the free energy of the probe brane and the phase transitions. The phase transition points can be determined from the thermodynamics of the probe brane. We interpret the on-shell action of Eq. (12) as a Helmholtz free energy [6]:

$$F_0(d) = \int_{u_h}^{\epsilon} \tilde{\mathcal{L}}(d)\mathrm{d}u. \tag{A1}$$

Since this integral is still divergent, we have to regularize it. According to [31], which is equivalent to the procedure in [5,6], the counterterms are given by

$$L_1 = \frac{1}{4}\mathcal{N}\sqrt{-\gamma}, \qquad L_2 = -\frac{1}{2}\mathcal{N}\sqrt{-\gamma}\theta(\epsilon)^2,$$
$$L_f = \mathcal{N}\frac{5}{12}\sqrt{-\gamma}\theta(\epsilon)^4, \tag{A2}$$

where γ is the induced metric at $z=\epsilon$ near the AdS boundary and $\sqrt{-\gamma} = \epsilon^{-4}$. Substituting $\theta(u) = \theta_0 u + \theta_2 u^2 + \cdots$, we obtain

$$L_1 = \frac{\mathcal{N}}{4}\frac{1}{\epsilon^4}, \quad L_2 = -\mathcal{N}\left(\frac{1}{2}\frac{\theta_0^2}{\epsilon^2} + \theta_0\theta_2\right), \quad L_f = \mathcal{N}\frac{5}{12}\theta_0^4. \tag{A3}$$

The coefficients θ_0 and θ_2 are related to the quark mass m_q and the quark condensate c by

$$\theta_0 = m_q, \qquad \theta_2 = c + \frac{1}{6}m_q^3, \tag{A4}$$

respectively. We write

$$\begin{aligned} L_{ct} &= L_1 + L_2 + L_f \\ &= \mathcal{N}\left[\frac{1}{4\epsilon^4} - \frac{m_q^2}{2\epsilon^2} - m_q\left(c + \frac{1}{6}m_q^3\right) + \frac{5}{12}m_q^4\right] \\ &= \mathcal{N}\int_{u_h}^{\epsilon}\left[-\frac{1}{u^5} + \frac{m_q^2}{u^3}\right]\mathrm{d}u + \mathcal{N}\left(\frac{1}{4u_h^4} - \frac{m_q^2}{2u_h^2}\right) \\ &\quad + \mathcal{N}\left(\frac{m_q^4}{4} - m_q c\right). \end{aligned} \tag{A5}$$

Then, the regularized free energy can be computed by

$$\begin{aligned} F &= \int_{u_h}^{\epsilon}\tilde{\mathcal{L}}\mathrm{d}u + L_{ct} = \int_{u_h}^{\epsilon}\left[\tilde{\mathcal{L}} + \mathcal{N}\left(-\frac{1}{u^5} + \frac{m_q^2}{u^3}\right)\right]\mathrm{d}u \\ &\quad + \mathcal{N}\left(\frac{1}{4u_h^4} - \frac{m_q^2}{2u_h^2} + \frac{m_q^4}{4} - m_q c\right). \end{aligned} \tag{A6}$$

In the multivalued region, $F(d)$ has swallowtail structure as a function of d, as shown in Fig. 5. In such cases, the intersection of the two branches of $F(d)$ is considered as a phase transition point.

The free energy is a thermodynamic potential in the canonical ensemble. In this case, d is treated as a controlling parameter. On the other hand, we can also consider the grand canonical ensemble setup when we treat μ as a controlling parameter. In the grand canonical ensemble, the thermodynamic potential is given by the grand potential

$$\Omega(\mu) = F - \mu d. \tag{A7}$$

Figure 6 shows Ω/T^4 as a function of $\tilde{\mu}$ at $\tilde{T} = 0.343737$. Note that there is the branch of the Minkowski embedding with vanishing density but finite μ. Considering both the Minkowski and BH embeddings, we can find swallowtail structure in $\Omega(\mu)$. The intersection point of the swallowtail in $\Omega(\mu)$ is the first order phase transition point. At low temperatures, the multivalued region of $\tilde{d}$ as a function of $\tilde{\mu}$ disappears. Then, $\tilde{d}$ goes zero at finite $\tilde{\mu}$ without the multivaluedness. It means the second order phase transition from the BH embedding to the Minkowski embedding.

The phase diagrams of the grand canonical and the canonical ensemble setups are shown in Fig. 2.

[1] J. M. Maldacena, The large N limit of superconformal field theories and supergravity, Adv. Theor. Math. Phys. **2**, 231 (1998).
[2] S. S. Gubser, I. R. Klebanov, and A. M. Polyakov, Gauge theory correlators from noncritical string theory, Phys. Lett. B **428**, 105 (1998).
[3] E. Witten, Anti-de Sitter space, thermal phase transition, and confinement in gauge theories, Adv. Theor. Math. Phys. **2**, 505 (1998).
[4] A. Karch and E. Katz, Adding flavor to AdS/CFT, J. High Energy Phys. 06 (2002) 043.
[5] S. Nakamura, Y. Seo, S.-J. Sin, and K. P. Yogendran, A new phase at finite quark density from AdS/CFT, J. Korean Phys. Soc. **52**, 1734 (2008).
[6] S. Nakamura, Y. Seo, S.-J. Sin, and K. P. Yogendran, Baryon-charge chemical potential in AdS/CFT, Prog. Theor. Phys. **120**, 51 (2008).
[7] D. Mateos, R. C. Myers, and R. M. Thomson, Holographic phase transitions with fundamental matter, Phys. Rev. Lett. **97**, 091601 (2006).
[8] D. Mateos, R. C. Myers, and R. M. Thomson, Thermodynamics of the brane, J. High Energy Phys. 05 (2007) 067.
[9] M. Kruczenski, D. Mateos, R. C. Myers, and D. J. Winters, Meson spectroscopy in AdS/CFT with flavor, J. High Energy Phys. 07 (2003) 049.
[10] J. Erdmenger, M. Kaminski, and F. Rust, Holographic vector mesons from spectral functions at finite baryon or isospin density, Phys. Rev. D **77**, 046005 (2008).
[11] R. C. Myers, A. O. Starinets, and R. M. Thomson, Holographic spectral functions and diffusion constants for fundamental matter, J. High Energy Phys. 11 (2007) 091.
[12] J. Mas, J. P. Shock, J. Tarrio, and D. Zoakos, Holographic spectral functions at finite baryon density, J. High Energy Phys. 09 (2008) 009.
[13] H. Liu, J. McGreevy, and D. Vegh, Non-Fermi liquids from holography, Phys. Rev. D **83**, 065029 (2011).
[14] T. Faulkner, H. Liu, J. McGreevy, and D. Vegh, Emergent quantum criticality, Fermi surfaces, and AdS(2), Phys. Rev. D **83**, 125002 (2011).
[15] N. Iqbal and H. Liu, Real-time response in AdS/CFT with application to spinors, Fortschr. Phys. **57**, 367 (2009).
[16] T. Faulkner, G. T. Horowitz, J. McGreevy, M. M. Roberts, and D. Vegh, Photoemission 'experiments' on holographic superconductors, J. High Energy Phys. 03 (2010) 121.
[17] E. Oh, T. Yuk, and S.-J. Sin, The emergence of strange metal and topological liquid near quantum critical point in a solvable model, J. High Energy Phys. 11 (2021) 207.
[18] E. Oh, Y. Seo, T. Yuk, and S.-J. Sin, Ginzberg-Landau-Wilson theory for flat band, Fermi-arc and surface states of strongly correlated systems, J. High Energy Phys. 01 (2021) 053.
[19] T. Yuk and S.-J. Sin, Flow equation and fermion gap in the holographic superconductors, J. High Energy Phys. 02 (2023) 121.
[20] D. Mateos, S. Matsuura, R. C. Myers, and R. M. Thomson, Holographic phase transitions at finite chemical potential, J. High Energy Phys. 11 (2007) 085.
[21] L. Martucci, J. Rosseel, D. Van den Bleeken, and A. Van Proeyen, Dirac actions for D-branes on backgrounds with fluxes, Classical Quantum Gravity **22**, 2745 (2005).
[22] I. Kirsch, Spectroscopy of fermionic operators in AdS/CFT, J. High Energy Phys. 09 (2006) 052.
[23] M. Ammon, J. Erdmenger, M. Kaminski, and A. O'Bannon, Fermionic operator mixing in holographic p-wave superfluids, J. High Energy Phys. 05 (2010) 053.
[24] R. Abt, J. Erdmenger, N. Evans, and K. S. Rigatos, Light composite fermions from holography, J. High Energy Phys. 11 (2019) 160.
[25] T. Nakas and K. S. Rigatos, Fermions and baryons as open-string states from brane junctions, J. High Energy Phys. 12 (2020) 157.
[26] A. Karch and A. O'Bannon, Holographic thermodynamics at finite baryon density: Some exact results, J. High Energy Phys. 11 (2007) 074.
[27] J. N. Laia and D. Tong, A holographic flat band, J. High Energy Phys. 11 (2011) 125.

[28] M. Cubrovic, J. Zaanen, and K. Schalm, String theory, quantum phase transitions and the emergent Fermi-liquid, Science **325**, 439 (2009).

[29] H. Wang, T. B. Park, S. Shin, H. Jang, E. D. Bauer, and T. Park, Field-induced multiple quantum phase transitions in the antiferromagnetic kondo-lattice compound $CeRhAl_4Si_2$, Phys. Rev. B **105**, 165110 (2022).

[30] A. Maurya, R. Kulkarni, A. Thamizhavel, D. Paudyal, and S. K. Dhar, Kondo lattice and antiferromagnetic behavior in quaternary $CeTAl_4Si_2$ (T = Rh, Ir) single crystals, J. Phys. Soc. Jpn. **85**, 034720 (2016).

[31] A. Karch, A. O'Bannon, and K. Skenderis, Holographic renormalization of probe D-branes in AdS/CFT, J. High Energy Phys. 04 (2006) 015.